OncoTargets and Therapy

Dovepress
open access to scientific and medical research

Open Access Full Text Article

ORIGINAL RESEARCH

RETRACTED ARTICLE: Histone Demethylase *KDM3A* Promotes Cervical Cancer Malignancy Through the *ETS1*/KIF14/Hedgehog Axis

This article was published in the following Dove Press journal:
OncoTargets and Therapy

Jinyu Liu[1,*]
Dongqing Li[2,*]
Xin Zhang[3]
Yanyan Li[1]
Jian Ou[4]

[1]Frist Department of Gynecologic Oncology, Jilin Cancer Hospital, Changchun 130012, Jilin, People's Republic of China; [2]Second Department of Gynecologic Oncology, Jilin Cancer Hospital, Changchun 130012, Jilin, People's Republic of China; [3]Department of Rheumatology and Immunology, China-Japan Union Hospital of Jilin University, Changchun 130033, Jilin, People's Republic of China; [4]Department of Gynecological Oncology Radiotherapy, Jilin Cancer Hospital, Changchun 130012, Jilin, People's Republic of China

*These authors contributed equally to this work

Background: Lysine demethylase 3A (*KDM3A*) has been increasingly recognized as an important epigenetic regulator involved in cancer development. This study aims to explore the relevance of *KDM3A* to cervical cancer (CC) progression and the molecules involved.

Materials and Methods: Tumor and the adjacent tissues from CC patients were collected. *KDM3A* expression in tissues and CC cell lines and its correlation with the survival and prognosis of patients were determined. Malignant potentials of CC cells and the angiogenesis ability of HUVECs were measured to evaluate the function of *KDM3A* on CC progression. The interactions among *KDM3A*, H3K9me2 and *ETS1*, and the binding between *ETS1* and *KIF14* were validated through ChIP and luciferase assays. Altered expression of *ETS1* and *KIF14* was introduced to explore their roles in CC development.

Results: *KDM3A* was abundantly expressed in CC tissues and cells and linked to dismal prognosis of CC patients. Knockdown of *KDM3A* suppressed malignant behaviors of CC cells. *KDM3A* was found to increase *ETS1* expression through the demethylation of H3K9me2. Overexpression of *ETS1* blocked the inhibiting roles of sh-KDM3A. *ETS1* could bind to the promoter region of *KIF14* to trigger its transcription. Overexpression of *KIF14* aggravated the malignant behaviors of CC cells and the angiogenesis ability of HUVECs and it activated the Hedgehog signaling pathway. Artificial activation of Hedgehog by Sag1.5 diminished the effects of sh-KDM3A. These changes were reproduced in vivo.

Conclusion: This study evidenced that *KDM3A* promotes *ETS1*-mediated *KIF14* transcription to promote CC progression with the involvement of the Hedgehog activation.

Keywords: lysine demethylase 3A, ETS proto-oncogene 1, kinesin family member 14, Hedgehog signaling pathway, cervical cancer

Introduction

Cervical cancer (CC) represents the fourth gynecological malignancy both in terms of incidence and mortality among females, with an estimated 570,000 diagnoses and 311,000 deaths in 2018 across the globe.[1] Specifically, the morbidity rate varies worldwide, with the highest rate in Eastern Africa and the lowest incidence in Western Asia; and it is the second most prevailing cancer in women in South East Asia.[2] Chemo- and radiotherapies are well recognized as the primary interventions for CC control, but the overall survival rate of the advanced patients who underwent these conventional therapies are still low, at about 40%.[3] Besides, the radiation exposure itself may bring side-effects and a risk fact for cancer development.[4]

Correspondence: Jian Ou
Department of Gynecological Oncology Radiotherapy, Jilin Cancer Hospital, No. 1018, Huguang Road, Changchun 130012, Jilin, People's Republic of China
Tel/Fax +86-18686500760
Email Oujian4184@163.com

Gene-based therapy has been accepted as a less-invasive promising approach that brings the development of many treating options focusing on different aspects,[5] which requires an increased understanding in the molecules of action.

Though initially less studied, the epigenetic mechanisms which mediate transcriptional regulation and dysregulation in cancer have aroused increasing focus among researchers in this field, mainly including the acetylation and methylation modifications.[6] Lysine demethylase 3A (*KDM3A*), also termed Jumonji domain-containing 1A (*JMJD1A*) and Jumonji C (domain-containing histone demethylase 2A) *JHDM2A*, is a histone H3 lysine 9 (H3K9) dimethyl and monomethyl (me2/1) demethylase has been implicated in many cellular processes from proliferation to progression, and is reported as an advanced target for cancer treatment.[7,8] But the role of *KDM3A* in CC development remains less concerned. Interestingly, a previous report suggested that *KDM3A* could interact-with the ETS proto-oncogene transcription factor 1 (*ETS1*) flanking its start site through a H3K9me2 demethylation manner, which leads to the further metastasis of Ewing sarcoma cells.[9] *ETS1* is a key member of the ETS domain family and is implicated in many essential processes in cancer development, such as invasion, epithelial-to-mesenchymal transition (EMT), drug-resist and angiogenesis.[10] Similarly, it was demonstrated as a promising therapeutic target for CC as well.[11] We therefore speculated that there is a similar interaction between *KDM3A* and *ETS1* in CC development. Moreover, A previous study noted that *ETS1* can promote the transcription activity of kinesin family member 14 (*KIF14*),[12] which has been documented to be abundantly expressed in CC and associated with chemo-resistance and unfavorable prognosis.[13] Therefore, we hypothesized that *ETS1* possibly regulates *KIF14* transcription to govern CC development. Hence this study performed in both cell and animal models to validate the functions of the above factors in CC progression and their interactions, as well as the potential pathway implicated.

Materials and Methods

Ethics Statement

The study was performed as per the Declaration of Helsinki and ratified by the Ethics Committee of Jilin Cancer Hospital. All patients signed an informed consent form before enrollment. The animal experimental protocol was approved by the Committee on the Ethics of Animal Experiments of Jilin Cancer Hospital. All animal procedures were performed in line with the Guide for the Care and Use of Laboratory Animals published by National Institutes of Health (NIH Publication No.85–23, revised 1996). Great efforts were made to reduce the usage and pain in animals.

Sample Collection

Tumor tissues and the adjacent tissues were collected from 50 CC patients who were treated in Jilin Cancer Hospital from January 2013 to April 2014. The first-time diagnosed patients with complete clinical information were free of any other malignancies or history of preoperative radiotherapy and chemotherapy. The tissues were collected during surgery and instantly preserved at −80°C. A 5-year follow-up study was performed.

Cell Transfection

An immortalized cervical epithelial cell line (H8) was from Cell Resource Center, the Chinese Academy of Sciences (Shanghai, China), and CC cell lines (HT-8, CaSki, HeLa and SiHa) were from American Type Culture Collection (ATCC, Manassas, VA, USA). All cells were cultivated in 10% fetal bovine serum (FBS)-supplemented DMEM containing 1% penicillin/streptomycin (all from Sigma-Aldrich Chemical Company, St Louis, MO, USA) at constant 37°C with 5% CO_2. The medium was refreshed every 3 days.

HeLa and SiHa cells were used for the following transfection. The short hairpin (sh) RNAs targeting KDM3A (sh-KDM3A1, 2#), overexpressing vector of ETS-1 (oe-ETS1) and KIF14 (oe-KIF14), and the corresponding control vectors were acquired from GenePharma Co., Ltd. (Shanghai, China). All transfection was performed in line with the protocols of a Lipofectamine 2000 kit (Thermo Fisher Scientific Inc., Waltham, MA, USA). A Hedgehog pathway-specific agonist Sag1.5 (HY-124,899) acquired from MedChemExpress (Monmouth Junction, NJ, USA) was used to activate the Hedgehog pathway in CC cells, and dimethyl sulphoxide (DMSO, Sigma-Aldrich) served as a control.

Reverse Transcription Quantitative Polymerase Chain Reaction (RT-qPCR)

An RNeasy Mini Kit (Qiagen Sciences, Valencia, CA, USA) was utilized to extract total RNA from cells or tissues. Then,

1.5 μg RNA was reversely transcribed to cDNA using the TaqMan Reverse Transcription Reagent (Applied Biosystems Inc., Carlsbad, CA, USA). Then, real-time qPCR was performed on a Prism 7900HT System (Applied Biosystems) and a SYBR Green PCR Master Mix (Applied Biosystems). The $2^{-\Delta\Delta Ct}$ method was used to determine gene expression. The primers are exhibited in Table 1, and *GAPDH* served as an internal reference.

Immunohistochemical (IHC) Staining

The tumor samples were fixed in paraformaldehyde, embedded in paraffin, cut into sections (4 μm), dewaxed, and rehydrated. Then, the sections were soaked in boiled 10 mM citrate buffer (pH=6.0) for 2 minutes of antigen retrieval, and then blocked with 100 μL H_2O_2 for 10 minutes. Then, the sections were co-cultured with the primary antibodies against KDM3A (1:50, ab91252, Abcam Inc., Cambridge, MA, USA), ETS1 (1:500, ab220361, Abcam), KIF14 (1:100, #PA5-87,769, Thermo Fisher) and Gli1 (1:200, #MA5-32,553, Thermo Fisher) at 4°C overnight, and then with the secondary antibodies anti-mouse IgG H&L (HRP) (ab205719, Abcam) and goat anti-rabbit IgG H&L (HRP) (ab6721, Abcam) at 20°C for 1 hour, followed by a 10-minute incubation with horseradish peroxidase (HRP)-labeled streptomycin (KIT-9710, MXB Biotechnologies, China). The staining was developed by 3.3'-diaminobenzidine, and the tissues were observed under a microscope (Nikon Eclipse NI, Japan).

Table 1 Primer Sequences for RT-qPCR

Gene	Primer Sequence (5'-3')
KDM3A	F: GCCAACATTGGAGA TTCTG R: CTCGAACACCTT GACAG TCG
ETS1	F: GAGTCAACC CA CTA CCAG R: GAGCGT GATAGC TCTGTG
KIF14	F: GCA TT GAACAAGC ACCA R: ATGTTGCTG AGCGGGACTAA
Bax	TCAGGATGCGTC CCAAGAAG R: TG TCCACGGCGGCAATCATC
Bcl2	TCGCC GTGGAGAACTACTGAGT R: C CA GAGAAATCAAACAGAGGC
E-cadherin	F: GCCTCCTGAAAAGAGAGTGGAAG R: TGGCAGTGTCTCTCCAAATCCG
N-cadherin	F: CCTCCAGAGTTTACTGCCATGAC R: GTAGGATCTCCGCCACTGATTC
Vimentin	F: AGGCAAAGCAGGAGTCCACTGA R: ATCTGGCGTTCCAGGGACTCAT
GAPDH	F: GTCTCCTCTGACTTCAACAGCG R: ACCACCCTGTTGCTGTAGCCAA

Abbreviations: RT-qPCR, reverse transcription quantitative polymerase chain reaction; KDM3A, lysine demethylase 3A; ETS-1, ETS proto-oncogene transcription factor 1; KIF14, kinesin family member 14; Bcl-2, B-cell lymphoma-2; Bax, Bcl-2-associated X; GAPDH, glyceraldehyde-3-phosphate dehydrogenase; F, forward; R, reverse.

Western Blot Analysis

Tissues and cells were collected by proteinase inhibitor-contained radio-immunoprecipitation assay (RIPA) cell lysis buffer on ice. After protein quantification by a bicinchoninic acid (BCA) kit (Pierce Waltham, MA, USA), an equal volume of protein lysates was separated by 8–12% SDS-PAGE and transferred onto PVDF membranes (Millipore, Billerica, MA, USA). Next, the membranes were blocked with 5% skimmed milk for 15 minutes and cultured with the primary antibodies against KDM3A (1:1,000, ab91252, Abcam), ETS1 (1:1,000, ab220361, Abcam), H3K9me2 (1:1,000, ab1220, Abcam), GAPDH (1:10,000, ab181602, Abcam), Gli1 (1:1,000, #MA5-32,553, Thermo Fisher), and Gli3 (1:1,500, ab81130, Abcam) at 4°C overnight, followed by 1 h incubation with the secondary antibodies anti-mouse IgG H&L (HRP) (ab205719, Abcam) and goat anti-rabbit IgG H&L (HRP) (ab6721, Abcam) at 20°C for 1 hour. Then, the blot bands were developed by enhanced chemiluminescence (ECL) reagent (Millipore) and scanned using an immune blotting system (Tanon 5200, China).

Cell Counting Kit-8 (CCK-8) Method

A CCK-8 kit was used to measure cell proliferation. Briefly, transfected cells were sorted into 96-well plates at 2,000 cells per well. Then, each well was loaded with 10 μL CCK-8 solution at different time points for another 2 hours of incubation at 37°C. The optical density (OD) at 450 nm was determined utilizing a spectrophotometer (Synergy H1, Bio-Tek, USA).

Colony Formation Assay

After transfection, cells were sorted in 6-well plates at 1×10^5 cells per well for 2 weeks of incubation. Then, the cells were immobilized in 4% paraformaldehyde for 30 minutes and stained with crystal violet (Sigma-Aldrich) for 15 minutes, and the number of colonies (over 50 cells) were observed under an inverted microscope (Olympus Optical Co., Ltd, Tokyo, Japan) with five random fields observed.

5-Ethynyl-2'-Deoxyuridine (EdU) Labeling Assay

A Cell-Light EdU DNA cell proliferation kit (RiboBio, Guangzhou, China) was used for DNA replication and proliferation measurement. Cells were sorted in 96-well plates at 2×10^4 cells per well. After 36 hours, each well was filled with 50 μM EdU solution for another 3 hours of incubation. Then, the cells were fixed and stained by Apollo solution. Nuclei were stained by 4', 6-diamidino-2-phenylindole (DAPI), and the staining images were captured under the inverted microscope. Five random fields were included, and the red staining (EdU-positive cells) and blue staining (DAPI-stained cells) were calculated.

Terminal Deoxynucleotidyl Transferase (TdT)-Mediated dUTP Nick End Labeling (TUNEL)

Apoptosis of cells was determined using a TUNEL kit from Beyotime Biotechnology Co., Ltd. (Shanghai, China). Briefly, cells were immobilized for 30 minutes and cultured in phosphate buffer saline (PBS) containing 0.3% Triton X-100 for 5 minutes of incubation. Then, the cells were additionally incubated with 50 μL fresh TUNEL reagent at 37°C avoiding light exposure for 60 minutes. Thereafter, the slides were anti-quenched by fluorescent mounting media, and the relative fluorescence intensity was determined by an EVOS FL microscope (Invitrogen, Thermo Fisher).

Flow Cytometry

An Annexin V-fluorescein isothiocyanate (FITC) apoptosis detection kit (Thermo Fisher) was used for apoptosis detection. Briefly, cells after transfection were centrifuged at 1,000 g for 5 minutes with the supernatant discarded. Next, the cells were resuspended in PBS, and the suspension containing 5×10^5 cells was centrifuged again to discard the supernatant, Then, the cells were resuspended in the Annexin V-FITC mixture and then stained with propidium iodide (PI) solution for 10–20 minutes of incubation at 20–25°C in dark condition. Cell apoptosis was evaluated using a flow cytometer (FACS Calibur, BD Biosciences, San Jose, CA, USA), and the data were analyzed by Flow J.

Wound-Healing Assay

Cells were sorted in 6-well plates. When the cell confluence reached 90–100%, a scratch was produced on the cells using a 200 μL pipette tip. Thereafter, the cells were cultured in FBS-free medium containing berberine chloride hydrate, an inhibitor for cancer cell growth (Gibco Company, Grand Island, NY, USA). The scratch width was measured at 0 and 48 hours using an inverted microscope (Olympus), and the migration rate of cells was evaluated by Image J.

Transwell Assay

Cell invasion was measured by a Transwell assay. The apical chambers (Millipore) were pre-coated with Matrigel (BD Biosciences). Then each apical chamber was filled with 200 μL serum-free cell suspension containing 1×10^5 transfected cells, while each basolateral chamber was added with 600 μL 10%FBS-DMEM. After 24 hours of incubation at 37°C, the non-invaded cells on the upper membrane were wiped out using cotton swabs, while the invaded cells were fixed for 30 minutes and stained by crystal violet for 20 minutes. The cells were observed under the inverted microscope, and the average value of five included fields of views was calculated.

Tube Formation Assay

A human umbilical vein endothelial cell (HUVEC) line purchased from ATCC was used for angiogenesis measurement. The cells were sorted in Matrigel-coated (90 μL) 24-well plates at 37°C for 30 minutes for polymerization, and then seeded into wells filled with different HeLa and SiHa cell-conditioned media. After a further 6 hours of incubation, the tube formation by HUVECs was imaged under the inverted microscope.

Immunofluorescence Staining

CC cells were fixed and permeated in 0.1%Triton X-100 for 30 minutes. After blockade by 5% skimmed milk, the cells were cultivated with anti-KDM3A (ab243641) and anti-ETS1 (ab186844) at 4°C overnight, and then with goat anti-rabbit IgG H&L (Alexa Fluor® 488) (ab150077) at 20°C for 1 hour. Then, the cells were rinsed and counterstained with 4',6-diamidino-2-phenylindole (DAPI, Sigma-Aldrich), and observed by a fluorescence microscope (Olympus). All antibodies were from Abcam.

Luciferase Reporter Assay

The putative binding sites between *ETS1* and the promoter region of *KIF14* were obtained from a bioinformatics system Jasper (http://jaspar.genereg.net/). The binding sites were PCR amplified and inserted to pGL3 vectors

(Promega, Corp., Madison, WI, USA) to construct *KIF14* promoter luciferase vectors (named Promoter). Then, the promoter was co-transfected with either oe-ETS1 or oe-NC into 293T cells (ATCC). Forty-eight hours later, the luciferase activity was determined using a Luciferase Reporter Assay System (Promega).

Chromatin Immunoprecipitation (ChIP) Assay

An EZ-Magna ChIP kit (EMD Millipore) was used to verify the interactions among *KDM3A*, and the promoter region of *ETS1* and *KIF14*. Briefly, CC cell lines were incubated in 1% formaldehyde solution for 15 minutes of crosslink and then quenched by glycine. Following ultrasonication, the DNA fragments were obtained. Specifically, for the binding relationship between *KDM3A* and *ETS1*, the promoter of *ETS1* was enriched by the magnet beads conjugated with anti-KDM3A in HeLa cells, while that was enriched by the magnet beads conjugated with anti-H3K9me2 in SiHa cells. For the binding relationship between *ETS1* and *KIF14*, the promoter of *KIF14* was enriched by the magnet-beads conjugated with anti-ETS1 in both HeLa and SiHa cells. Magnet beads conjugated with IgG served as a control. The precipitated chromatin DNA was analyzed by RT-qPCR.

Xenograft Tumor in Nude Mice

Twenty NU-Foxn1^{nu} mice (4–6 weeks old) were from Vital River Laboratory Animal Technology Co., Ltd. (Beijing, China). HeLa and SiHa cells with stable sh-KDM3A or sh-NC transfection were implanted into the mice through a subcutaneous injection. From the 10th day after cell implantation, the tumor size was measured using a vernier caliper every 5 days. The tumor volume (V) was determined as follows: V=length×width^2×0.52. The mice were euthanized through an overdose of pentobarbital

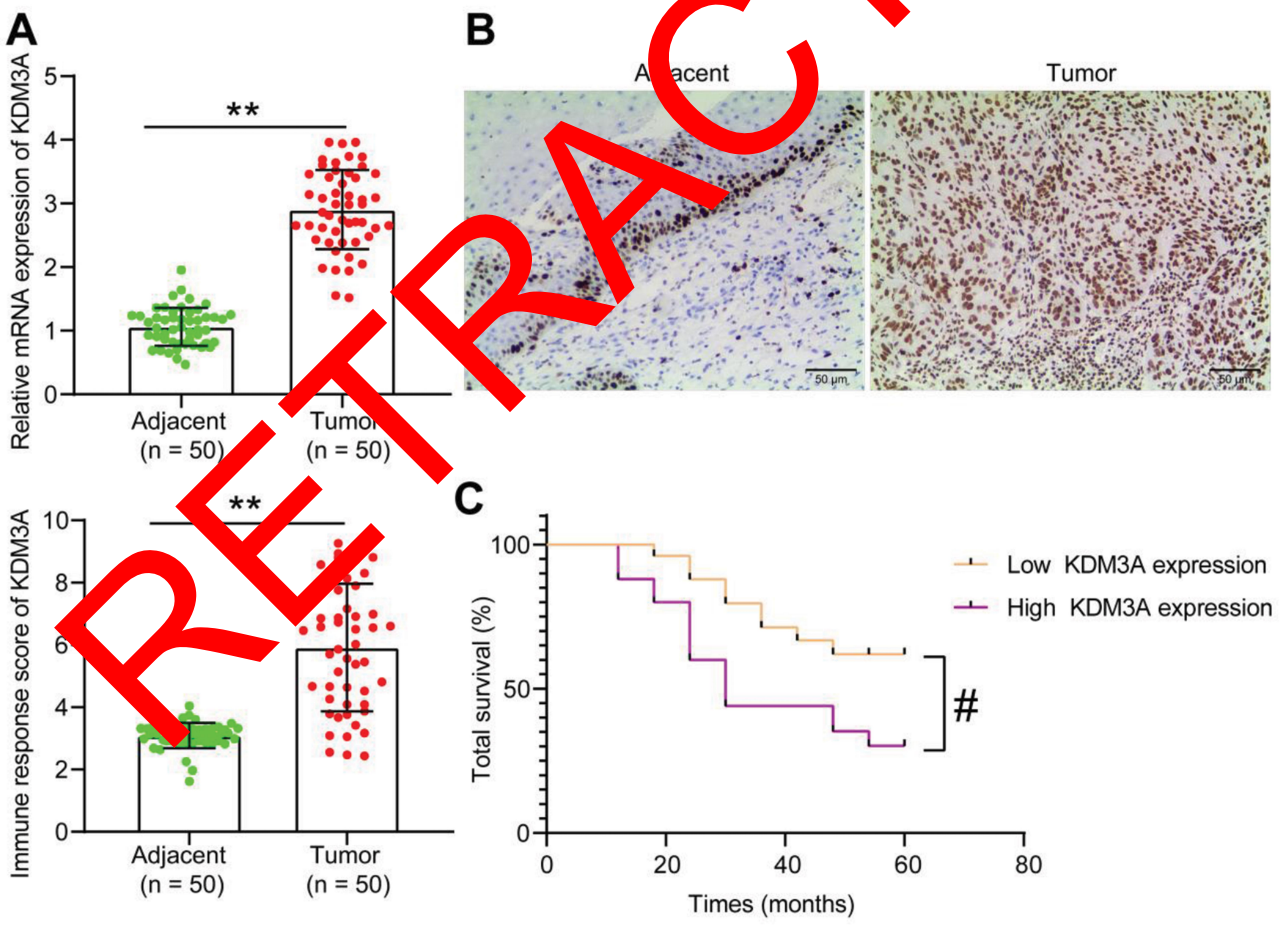

Figure 1 *KDM3A* is abundantly expressed in CC and indicates a dismal prognosis in patients. (**A**) mRNA expression of *KDM3A* in CC and adjacent tissues determined by RT-qPCR (n=50); (**B**) staining intensity of *KDM3A* in CC tumor and the adjacent tissues by IHC staining (n=50); (**C**) correlation between *KDM3A* expression and the 5-year survival rate in CC patients. In panels (**A**) and (**B**), data were analyzed by paired *t* test, $^{**}P<0.01$; in panel (**C**), correlation was analyzed by the Log-rank (Mantel-Cox) test, $^{\#}P<0.05$.

sodium (150 mg/kg, intraperitoneal injection) on the 30th day. Then, the tumors were collected and weighed for histological examination.

Statistical Analysis

Prism 8.0 (GraphPad, La Jolla, CA, USA) was used for data analysis. Data were obtained from no less than three independent experiments and presented as mean±standard deviation (SD). Differences were analyzed by paired *t*-test (two groups) and one-way or two-way analysis of variance (ANOVA), followed by Tukey's multiple test (over two groups). The Log-rank (Mantel-Cox) test was used to record the survival rate of patients. Enumeration data were analyzed by Fisher's exact test. The correlations between variables were evaluated by Spearman's rank correlation coefficient. *$P<0.05$ represents statistical significance.

Results

KDM3A is Abundantly Expressed in CC Tissues and Indicates a Dismal Prognosis in Patients

Though the oncogenic roles of *KDM3A* have been mentioned, its function in CC remains largely unknown. Here, we first examined mRNA expression of *KDM3A* in the tumor tissues and the paired adjacent tissues from 30 CC patients, which suggested that the *KDM3A* expression in CC tissues was increased (Figure 1A). Based on this, the following IHC staining results showed that the staining intensity of *KDM3A* was higher in tumor tissues than in the adjacent tissues (Figure 1B). According to the average value (2.9) of *KDM3A* expression in tumor tissues, the included patients were allocated into the high *KDM3A* expression group (n=25) and poor *KDM3A* expression group (n=25). It was found that CC patients with higher *KDM3A* expression had a significantly worse 5-year survival rate (Figure 1C). The clinical characteristics of patients are exhibited in Table 2, which suggested that a high *KDM3A* expression profile in patients was correlated with worse clinical presentation, such as increased lymphatic metastasis, while there was limited tumor differentiation.

Knockdown of *KDM3A* Suppresses CC Cell Growth

Following the findings above, we then measured expression of *KDM3A* in H8 and CC cell lines (HT-8, CaSki, HeLa, and SiHa). It was found that the mRNA and protein expression of KDM3A was notably increased in CC cell lines compared to that in H8 cells (Figure 2A and B). The HeLa and SiHa cells, owning the highest *KDM3A* expression, were chosen for the following experiments.

Next, sh-KDM3A 1# and sh-KDM3A 2# were transfected into HeLa and SiHa cells, and they both showed effective interference on KDM3A expression (Figure 2C and D). The sh-KDM3A 1# with a better interfering efficacy was chosen for further experiments. After

Table 2 Correlations Between the Clinicopathologic Characteristics and *KDM3A* Expression in Patients with Cervical Cancer (n=50)

Clinical Variables	Cases (n=50)	*KDM3A* Expression		*P*-value
		Low (n=25)	High (n=25)	
Age	≥45 (n=37) <45 (n=13)	21 (56.76%) 4 (30.77%)	16 (43.24%) 9 (69.23%)	0.1963
Tumor size	≥4 cm (n=21) <4 cm (n=29)	12 (38.71%) 13 (44.83%)	19 (61.29%) 16 (55.17%)	0.7938
Lymphatic metastasis	Yes (n=12) No (n=38)	2 (16.67%) 23 (60.53%)	10 (83.33%) 15 (39.47%)	0.0181*
Differentiation Grade	Well (n=14) Moderate (n=24) Poor (n=12)	11 (78.57%) 14 (58.33%) 3 (25%)	3 (21.43%) 10 (41.67%) 9 (75%)	0.0221*
FIGO stage	Stage I (n=17) Stage II (n=33)	11 (64.71%) 13 (39.39%)	6 (35.29%) 20 (60.61%)	0.1359

Notes: Enumeration data were analyzed by Fisher's exact test; *$P<0.05$.
Abbreviations: *KDM3A*, lysine demethylase 3a; FIGO, Federation of Gynecology and Obstetrics.

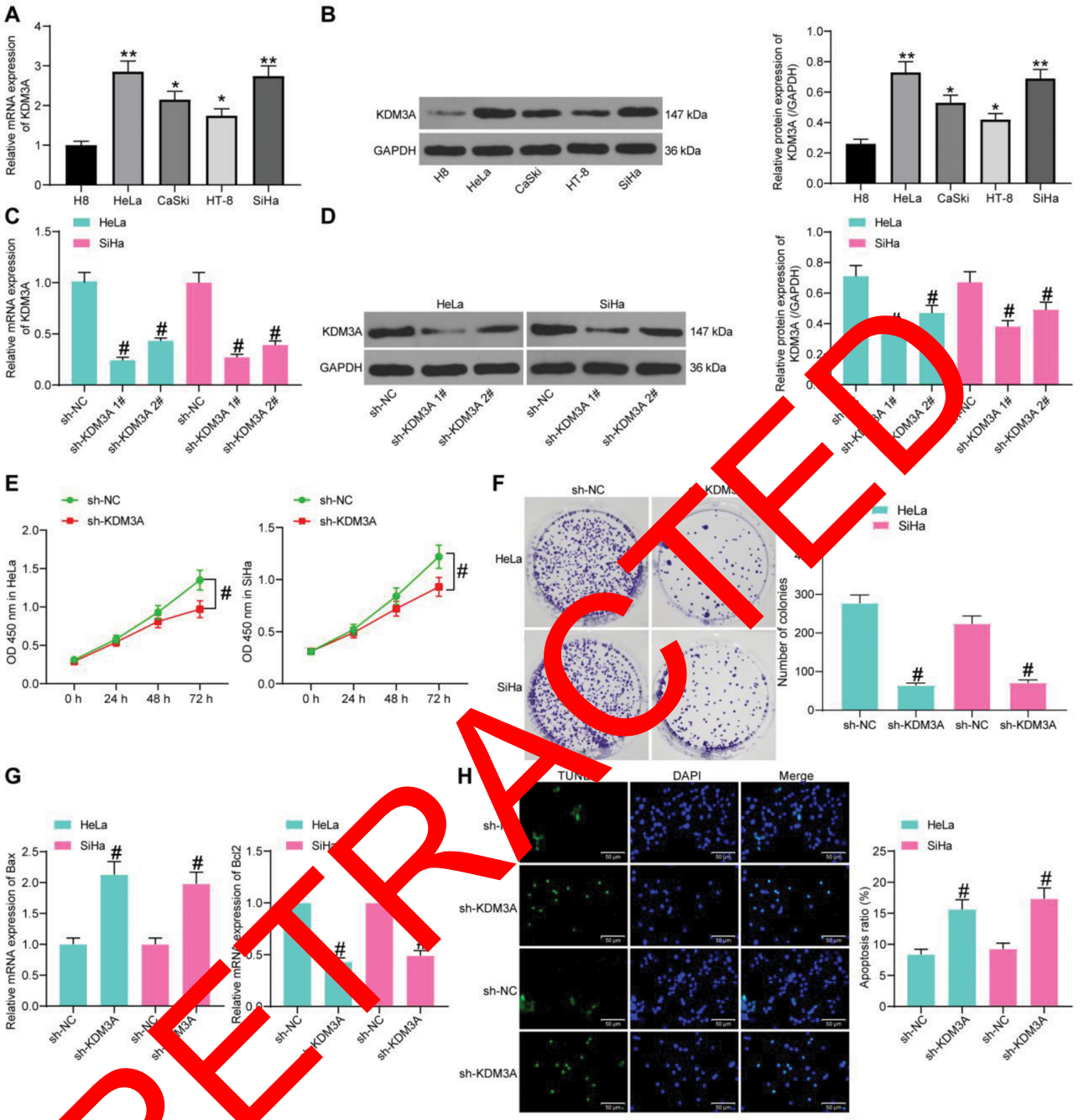

Figure 2 Knockdown of *KDM3A* suppresses CC cell growth. mRNA (**A**) and protein (**B**) expression of KDM3A in H8 and CC cell lines (HT-8, CaSki, HeLa, and SiHa) determined by RT-qPCR and Western blot analysis, respectively; mRNA (**C**) and protein (**D**) expression of KDM3A in HeLa and SiHa cells after sh-KDM3A 1# and sh-KDM3A 2# transfection measured by T-qPCR and Western blot analysis, respectively; (**E**) proliferation of CC cells determined by the CCK-8 method; (**F**) colony formation ability of CC cells; (**G**) expression of apoptosis-related factors Bax and Bcl-2 in CC cells determined by RT-qPCR; (**H**) apoptosis rate of CC cells determined by TUNEL. In panels (**A–D, F–H**), data were analyzed by one-way ANOVA, while data in panel (**E**) were analyzed by two-way ANOVA, followed by Tukey's multiple comparison test. **P*<0.05, ***P*<0.01 compared to H8; #*P*<0.05 compared to sh-NC.

KDM3A knockdown, the proliferation ability according to the CCK-8 assay, and the colony formation ability of cells were notably reduced (Figure 2E and F). As for cell apoptosis, the RT-qPCR results identified an increase in *Bax* (pro-apoptotic) expression, with a decline in *Bcl-2* (anti-apoptotic) expression upon *KDM3A* knockdown (Figure 2G). More obviously, the TUNEL staining results showed that the apoptosis rate of cells was notably enhanced after sh-KDM3A administration (Figure 2H).

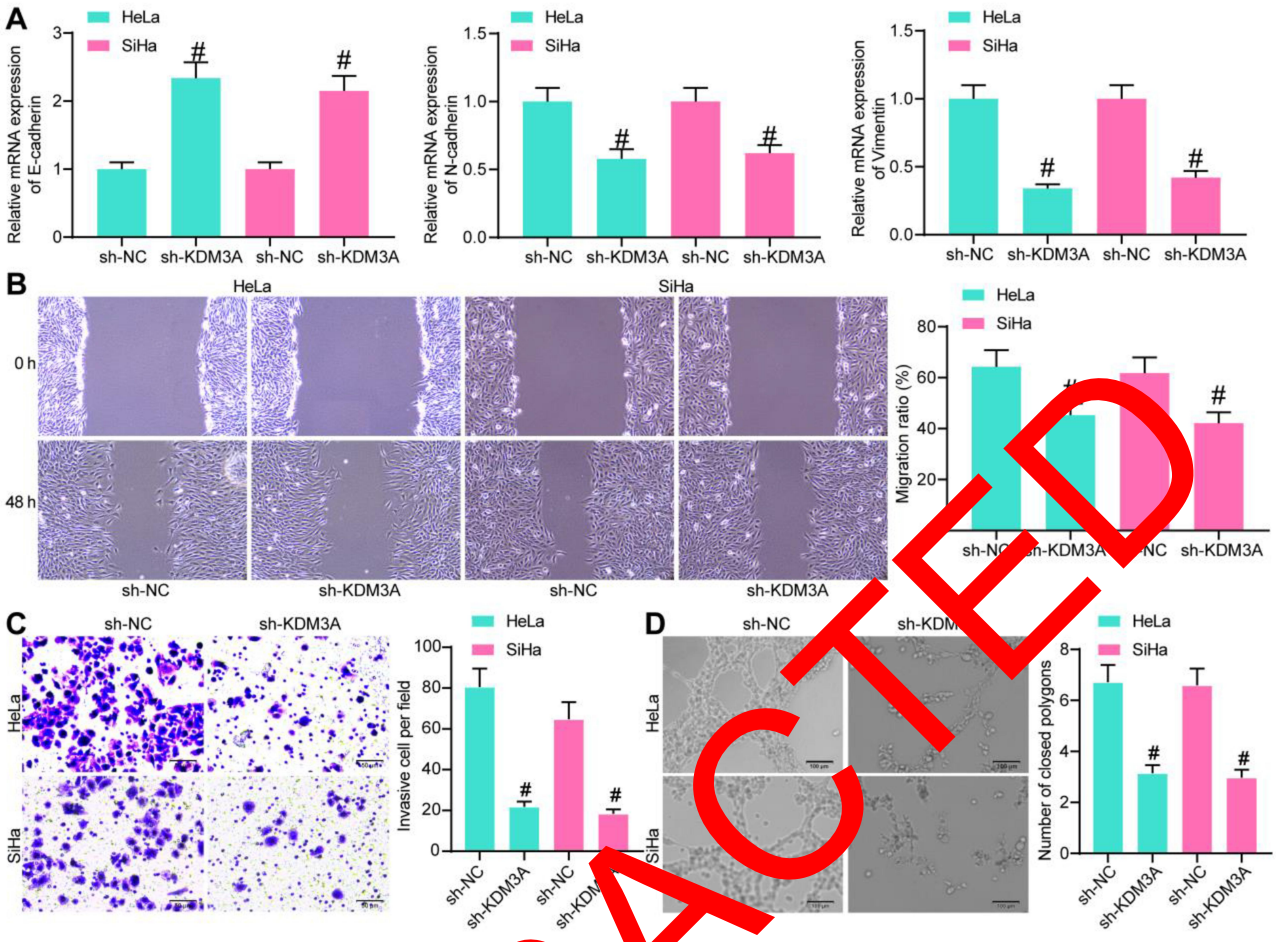

Figure 3 Knockdown of *KDM3A* inhibits metastasis of CC cells and angiogenesis by HUVECs. (**A**) Expression of EMT-related factors in HeLa and SiHa cells determined by RT-qPCR; (**B**) migration ability of CC cells evaluated by a wound-healing assay; (**C**) invasion ability of CC cells measured by a Transwell assay; (**D**) angiogenesis ability of HUVECs in different conditioned medium determined by a tube formation assay. In all panels, data were compared by one-way ANOVA. $^{\#}P<0.05$ compared to sh-NC.

Knockdown of *KDM3A* Inhibits Metastasis of CC Cells and Angiogenesis by HUVECs

We further explored the relevance of *KDM3A* with the metastasis of CC cells. First, expression of the EMT-related factors was measured by RT-qPCR, which identified an increase in E-cadherin while a decline in the expression of N-cadherin and Vimentin in *KDM3A* knockdown (Figure 3A). In addition, the wound healing assay results suggested that the migration of cells was notably decreased when *KDM3A* was suppressed (Figure 3B). Similarly, the invasive potential of CC cells was reduced following *KDM3A* downregulation (Figure 3C). These collectively showed that knockdown of *KDM3A* suppressed metastasis of CC cells. In addition, a tube formation assay was performed by seeding HUVECs in different HeLa and SiHa cell-conditioned medium, which showed that the number of formed tubes by HUVECs was declined after *KDM3A* knockdown (Figure 3D).

KDM3A Activates *ETS1* Through Demethylation of H3K9me2

As discussed above, we hypothesized that *KDM3A* possibly mediated *ETS1* activity through the demethylation and histone modification of H3K9me2. Thereafter, we first explored ETS1 expression in the collected CC tissues. The RT-qPCR results suggested that the mRNA expression of *ETS1* was notably increased in tumor tissues relative to the paired adjacent tissues (Figure 4A) and shared a positive correlation with *KDM3A* expression (Figure 4B). Again, the IHC staining showed an increased positive expression of *KDM3A* in tumor tissues (Figure 4C).

In HeLa and SiHa cells, we identified that both *KDM3A* and *ETS1* were sub-localized in nuclear according to the immunofluorescence staining (Figure 4D). Then, *ETS1* expression in CC cells with stable sh-KDM3A transfection was determined by RT-qPCR, which showed that

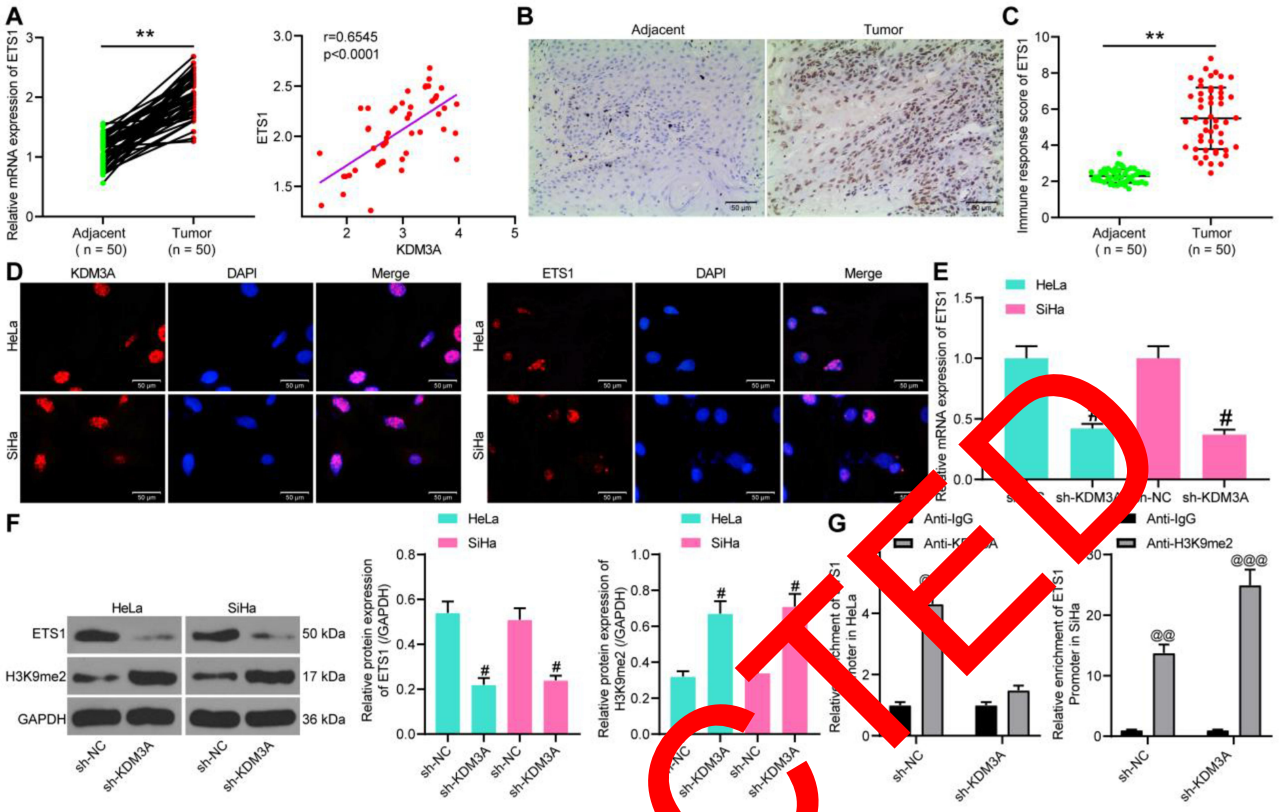

Figure 4 *KDM3A* activates *ETS1* through demethylation of H3K9me2. (**A**) *ETS1* expression in tumor tissues and the paired adjacent tissues determined by RT-qPCR; (**B**) a positive correlation between *KDM3A* and *ETS1* expression; (**C**) *ETS1* expression in tumor and adjacent tissues evaluated by IHC staining; (**D**) subcellular localization of *ETS1* and *KDM3A* in cells determined by immunofluorescence staining; (**E**) mRNA expression of *ETS1* in cells determined by RT-qPCR; (**F**) protein expression of ETS1 and H3K9me2 in cells after sh-KDM3A administration determined by Western blot analysis; (**G**) interactions among *KDM3A*, H3K9me2, and ETS1 promoter determined by ChIP assays. In panels (**A** and **C**), data were compared by the paired *t*-test, $^{**}P<0.05$ compared to Adjacent; in panel (**B**), correlation was evaluated by Spearman's rank correlation coefficient, r=0.6545, $P<0.0001$; data in panels (**E** and **F**) were compared by one-way ANOVA, while in panel (**G**) by two-way ANOVA, followed by Tukey's multiple comparison test, $^{\#}P<0.05$ compared to sh-KDM3A; $^{@@}P<0.01$, $^{@@@}P<0.001$ compared to anti-IgG.

sh-KDM3A notably inhibited *ETS1* expression in cells (Figure 4E). Likewise, the protein expression of ETS1 in cells was decreased as well after sh-KDM3A administration (Figure 4F), and, interestingly, the protein level of H3K9me2 in cells was notably increased (Figure 4F). Thereafter, a ChIP assay was performed to validate the regulatory network between *KDM3A* and *ETS1* (Figure 4G). In HeLa cells, compared to anti-IgG, an enrichment of *ETS1* promoter sequence was found in the immunoprecipitates combined by anti-KDM3A. Following sh-*KDM3A* administration, the enrichment of *ETS1* promoter sequence in the precipitates by anti-KDM3A was notably reduced. In SiHa cells, we found that, compared to anti-IgG, anti-H3KPme2 enriched the *ETS1* promoter sequence in the precipitates, while this enrichment was further strengthened upon *KDM3A* knockdown. These results showed that *KDM3A* promotes *ETS1* transcription through the demethylation and histone modification of H3K9me2.

Overexpression of *ETS1* Blocks the Inhibition of Sh-KDM3A on CC Cells

To validate the implication of ETS1 in the KDM3A mediation, overexpression of ETS1 was further introduced into CC cells in the presence of KDM3A knockdown, and the transfection efficacy was, again, confirmed by RT-qPCR and Western blot assays (Figure 5A and B). Then, the CCK-8 method showed that the proliferation of cells suppressed by sh-KDM3A was recovered upon *ETS1* overexpression (Figure 5C). Next, the flow cytometry suggested that the apoptosis rate of cells was reduced by the further upregulation of *ETS1* (Figure 5D). In addition, the migration and invasion abilities of cells reduced by sh-KDM3A were recovered upon *ETS1* overexpression (Figure 5E and F). Moreover, HUVECs were sorted in the conditioned medium of CC cells with stable transfection of oe-*ETS1*, after which the angiogenesis ability of cells suppressed by sh-KDM3A was notably recovered (Figure 5G).

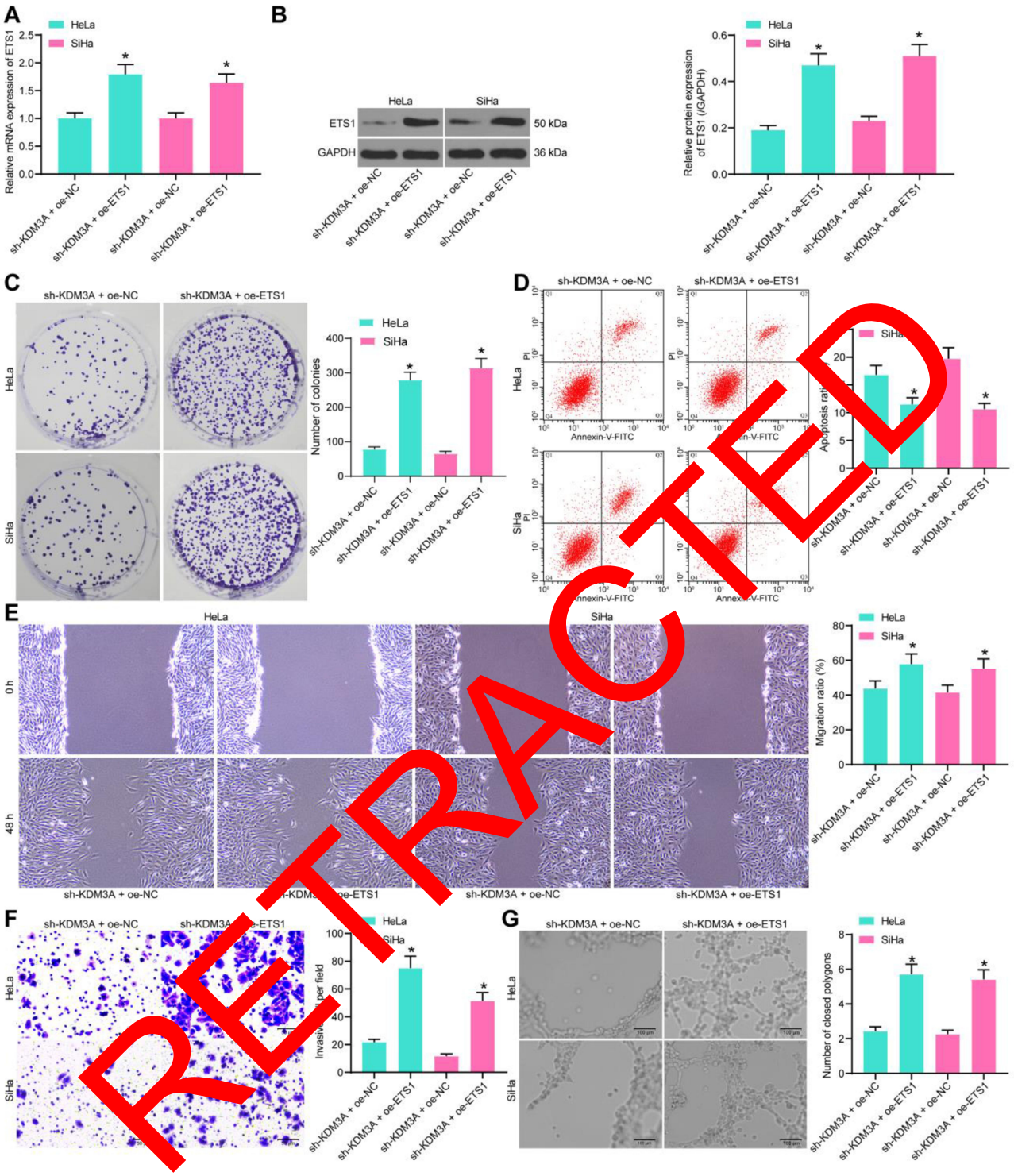

Figure 5 Overexpression of ETS1 blocks the inhibition of sh-KDM3A on CC cells. (**A** and **B**) Transfection efficacy of oe-ETS1 in cells determined by RT-qPCR and Western blot analysis, respectively; (**C**) proliferation ability of cells measured by colony formation assay; (**D**) apoptosis rate of cells measured after ETS1 overexpression determined by flow cytometry; migration (**E**) and invasion (**F**) abilities of cells determined by wound-healing and Transwell assays, respectively; (**G**), angiogenesis ability of cells determined by tube formation assay. Data were analyzed by one-way ANOVA, followed by Tukey's multiple comparison. *P<0.05 compared to sh-KDM3A+oe-NC.

ETS1 Transcriptionally Activates *KIF14*

As mentioned above, *ETS1* has been reported to transcriptionally activate *KIF14*,[12] an oncogene in CC.[13] First, mRNA expression of *KIF14* in the collected tissues from CC patients was determined, which exhibited that the KIF14 expression was notably increased in the tumor

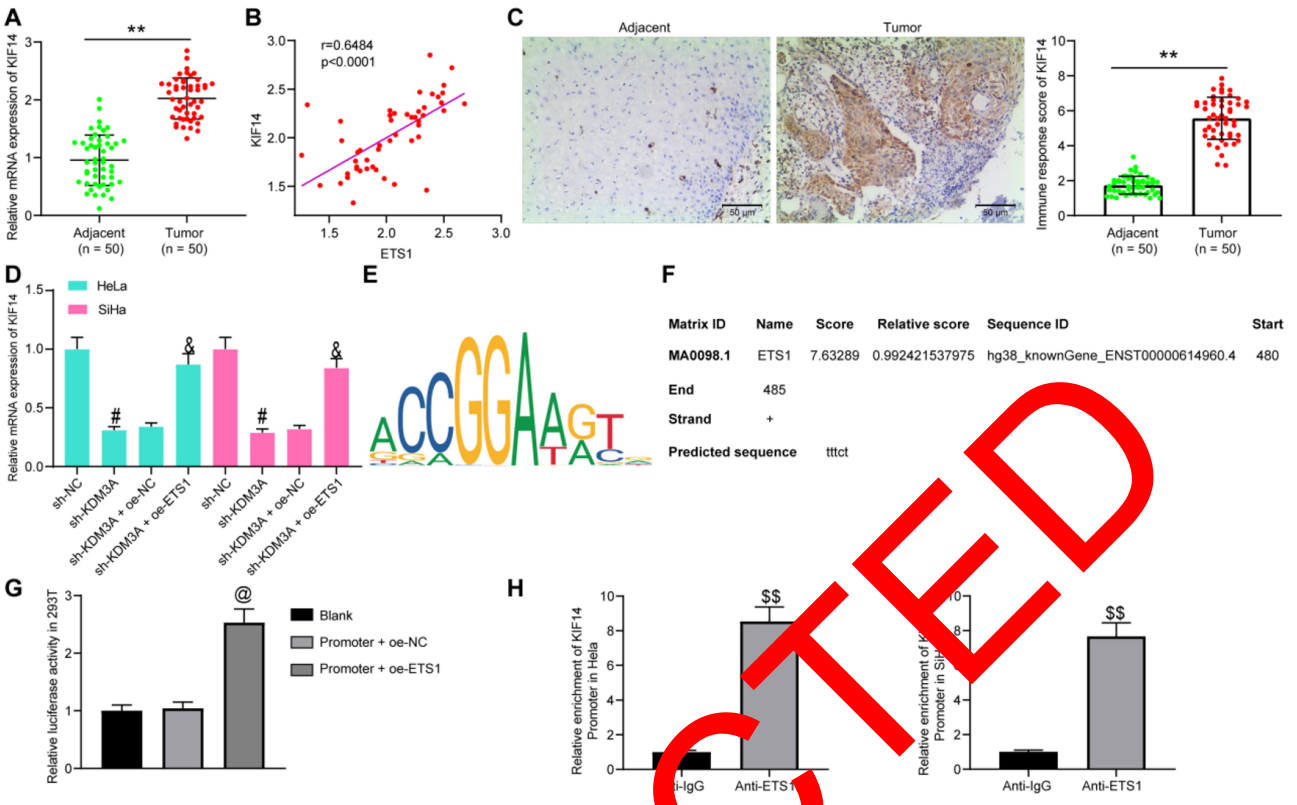

Figure 6 *ETS1* transcriptionally activates *KIF14*. (**A**) *KIF14* expression in tumor and adjacent tissues determined by RT-qPCR; (**B**) a positive correlation between *ETS1* and *KIF14* expression; (**C**) *KIF14* expression in tumor and adjacent tissues measured by IHC staining; (**D**) *KIF14* expression in HeLa and SiHa cells after sh-KDM3A or oe-ETS1 administration determined by RT-qPCR; (**E**) putative binding sites between *ETS1* and *KIF14* predicted on Jaspar; (**F**), the binding site with highest score used for luciferase assay; (**G** and **H**), binding relationship between *ETS1* and *KIF14* Promoter validated by luciferase and ChIP (**H**) assay. In panels (**A** and **C**), data were analyzed by paired *t*-test while data in panel (**H**) by unpaired *t*-test, $^{**}P<0.01$ compared to Adjacent, $^{\$\$}P<0.01$ compared to anti-IgG; in panel (**B**), correlation was evaluated by Spearman's rank correlation coefficient, r=0.6484, $P<0.0001$; data in panels (**D** and **G**) were compared by two-way ANOVA, $^{\#}P<0.05$ compared to sh-NC, $^{\&}P<0.05$ compared to sh-KDM3A+oe-NC, $^{@}P<0.05$ compared to Promoter+oe-NC.

tissues compared to the matched adjacent tissues (Figure 6A) and positively associated with *ETS1* expression (Figure 6B). Again, the IHC staining intensity of *KIF14* was notably enhanced in tumor tissues (Figure 6C).

We then measured mRNA expression of *KIF14* in cells after different transfection and it was found that the KIF14 expression was decreased by sh-KDM3A but then recovered by the further administration of oe-ETS1 (Figure 6D). Then, the putative binding sites between *ETS1* and the promoter region of *KIF14* were predicted on Jaspar (http://jaspar.genereg.net/) (Figure 6E). Then, the binding site with the highest score (Figure 6F) was selected for luciferase assay to validate the binding relationship. The Promoter was co-transfected with oe-NC or oe-ETS1 in 293T cells. After 48 hours, the luciferase activity of Promoter was notably increased by oe-ETS1 (Figure 6G). In addition, a ChIP assay was performed, which found an enrichment of *KIF14* promoter was found in the precipitates by anti-ETS1 (Figure 6H), indicating a direct binding relationship between *ETS1* and the promoter of *KIF14*.

KIF14 Activates the Hedgehog Signaling Pathway and Promotes CC Progression

*KIF14*has been documented as a positive regulator of the Hedgehog signaling pathway,[14] whose activation may lead to further development of CC.[15,16] To explore whether *KIF14* mediates this signaling pathway in CC, oe-KIF14 was administrated into CC cells, and the successful transfection was validated by RT-qPCR (Figure 7A). Then, the expression of Hedgehog-signaling marker proteins Gli1 and Gli3 was measured by Western blot analysis, which suggested that *KIF14* led to a notable increase in the expression of the two proteins (Figure 7B), namely, activating the Hedgehog signaling pathway.

Further, the EdU labeling assay results showed that the EdU-positive rate in CC cells was increased by oe-KIF14 (Figure 7C), while the apoptosis rate of cells was reduced (Figure 7D). In addition, the migratory and invasive potentials of CC cells were promoted upon KIF14 upregulation (Figure 7E and F). Moreover, the angiogenesis ability of

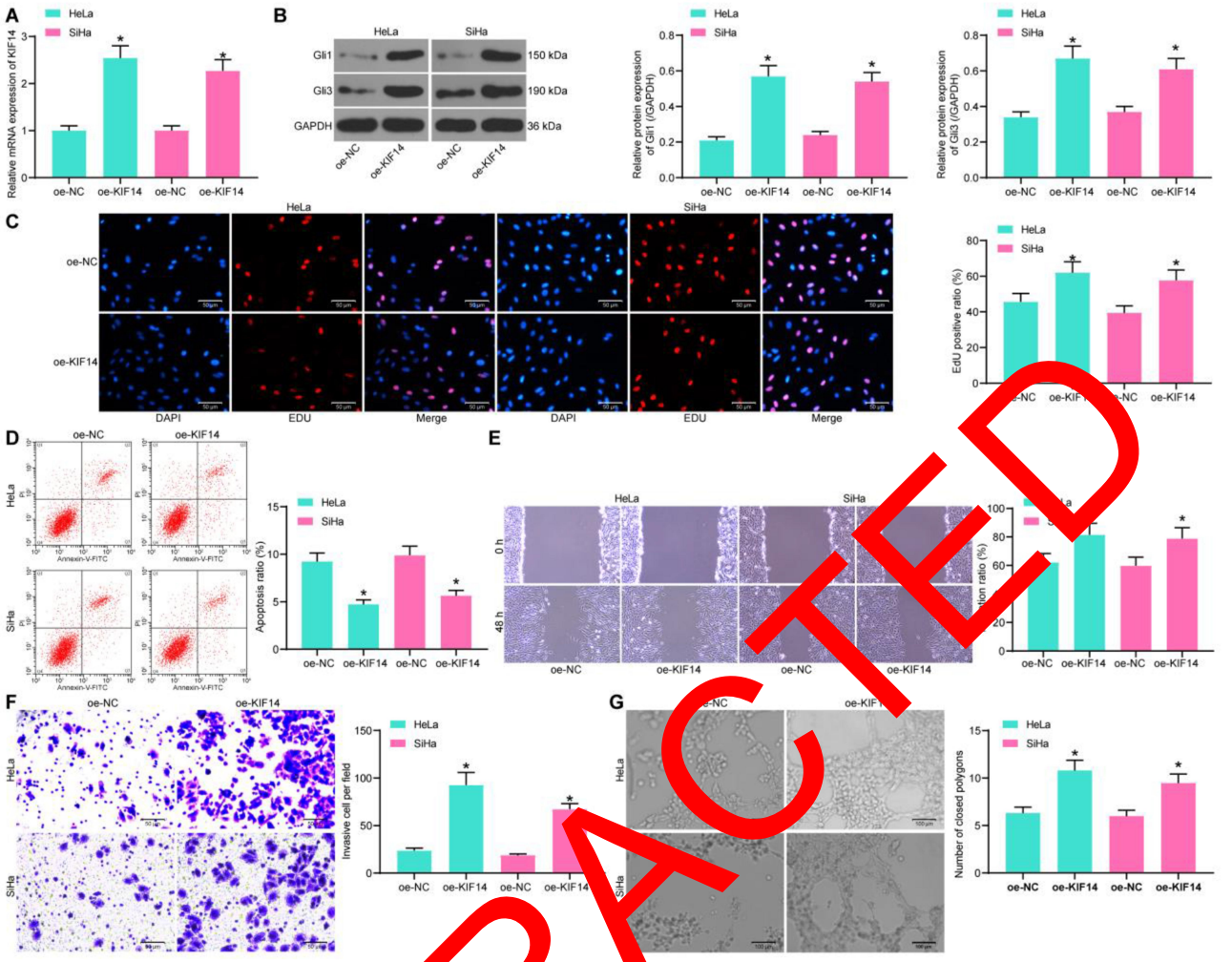

Figure 7 KIF14 activates the Hedgehog signaling pathway and promotes CC progression. (**A**) Transfection efficacy of oe-KIF14 determined by RT-qPCR; (**B**) protein levels of Gli1 and Gli3 in cells determined by Western blot analysis; (**C**) DNA replication in cells determined by EdU staining; (**D**) apoptosis rate in cells determined flow cytometry; migration (**E**) and invasion (**F**) abilities of cells determined by wound-healing and Transwell assays; (**G**) angiogenesis ability of HUVECs determined by tube formation assay. Data were analyzed by one-way ANOVA, *P < 0.05 compared to oe-NC.

HUVECs cultivated in conditioned medium with stable transfection of oe-KIF14 was increased (Figure 7G).

Activation of Hedgehog Blocks the Inhibitive Role of Sh-KDM3A in CC

To further validate the involvement of Hedgehog in the above events, a rescue experiment was performed through additional administration of a Hedgehog-specific agonist Sag1.5 in cells pre-treated with sh-KDM3A. Then, it was found that this signaling pathway was notably activated (Figure 8A). Thereafter, the colony formation assay results showed that the proliferation of HeLa and SiHa cells inhibited by sh-KDM3A was recovered by Sag1.5 (Figure 8B). In addition, the promotion on cell apoptosis, and the suppression of sh-KDM3A on cell migration and invasion as well as angiogenesis ability of HUVECs were all blocked by the further usage of Sag1.5 (Figure 8C–F). These results indicated that Hedgehog is a important downstream effector of *KDM3A* in CC progression.

Sh-KDM3A Suppresses Tumor Growth in vivo

HeLa and SiHa cells with stable sh-KDM3A transfection were implanted into the ventral side of mice through a subcutaneous injection. The tumor volume was recorded since the 10th day at a 5-day interval (Figure 9A), which showed that knockdown of *KDM3A* suppressed growth of xenograft tumors in mice. On the 30th day, the mice were euthanized and the tumor tissues were collected and weighed. Again, the tumor weight was reduced upon *KDM3A* knockdown (Figure 9B). Furthermore, the IHC staining results showed that the staining intensity of

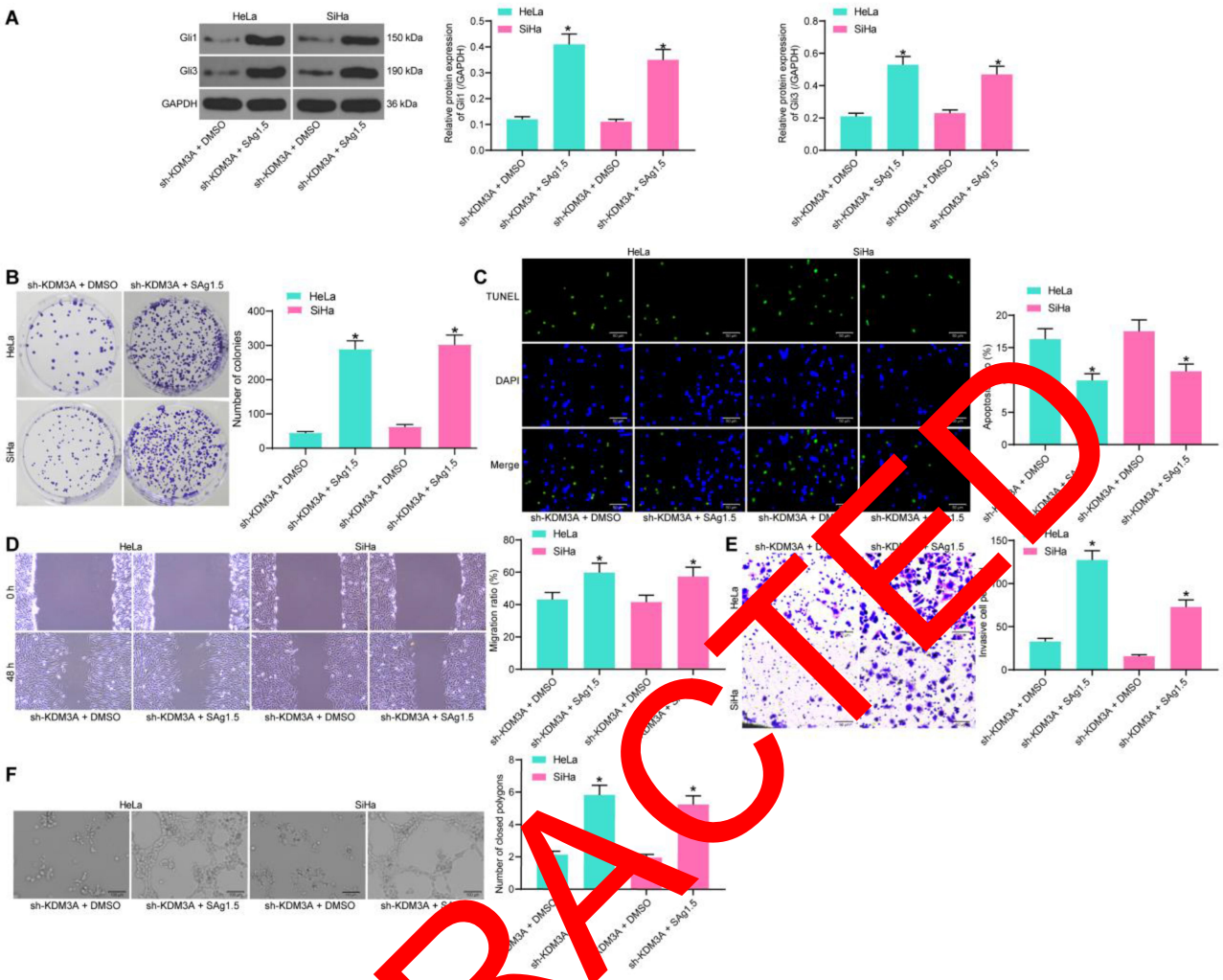

Figure 8 Activation of Hedgehog blocks the inhibiting role of sh-KDM3A in CC. (**A**) Protein levels of Gli1 and Gli3 in cells determined by Western blot analysis; (**B**) proliferation of CC cells determined by colony formation assay; (**C**) apoptosis rate of cells measured by TUNEL assay; migration (**D**) and invasion (**E**) abilities of cells determined by wound-healing and Transwell assays; (**F**) angiogenic ability of HUVECs determined by tube formation assay. Data were analyzed by one-way ANOVA, **P*<0.05 compared to sh-KDM3A+DMSO.

KDM3A, *ETS1*, *KIF14*, Gli1, and Gli3 was notably reduced in the tumor tissues from mice implanted with cells with stable sh-KDM3A transfection (Figure 9C). These results showed that sh-KDM3A suppresses tumor growth in vivo.

Discussion

As a leading cause of cancer related death among females, CC remains a huge healthy concern in the modern society, especially in those low-income countries,[2] owing to the current limitation in effective treatments. Researchers have made great efforts to explore novel molecular mechanisms and to develop promising factors with prognostic or therapeutic values to overcome the typical malignant behaviors from proliferation to metastasis.[17–19] Methylation of histone lysine is crucial for epigenetic correlated gene expression profiles in cancer.[20] In this study, we validated an interaction network involving *KDM3A*/*ETS1*/*KIF14*, in which *KDM3A* governs *ETS1*-mediated *KIF14* transcription to promote CC growth in either cell and animal models with the further involvement of the Hedgehog signaling pathway.

The *KDM3A* has been reviewed as a promising target for human cancer treatment.[8] Its oncogenic role has been well demonstrated.[21–23] Here, the initial finding of the current study was that *KDM3A* was highly expressed in the collected tumor tissues from CC patients, and it led to a dismal 5-year survival rate, increased lymphatic metastasis, and decreased tumor differentiation rate in patients.

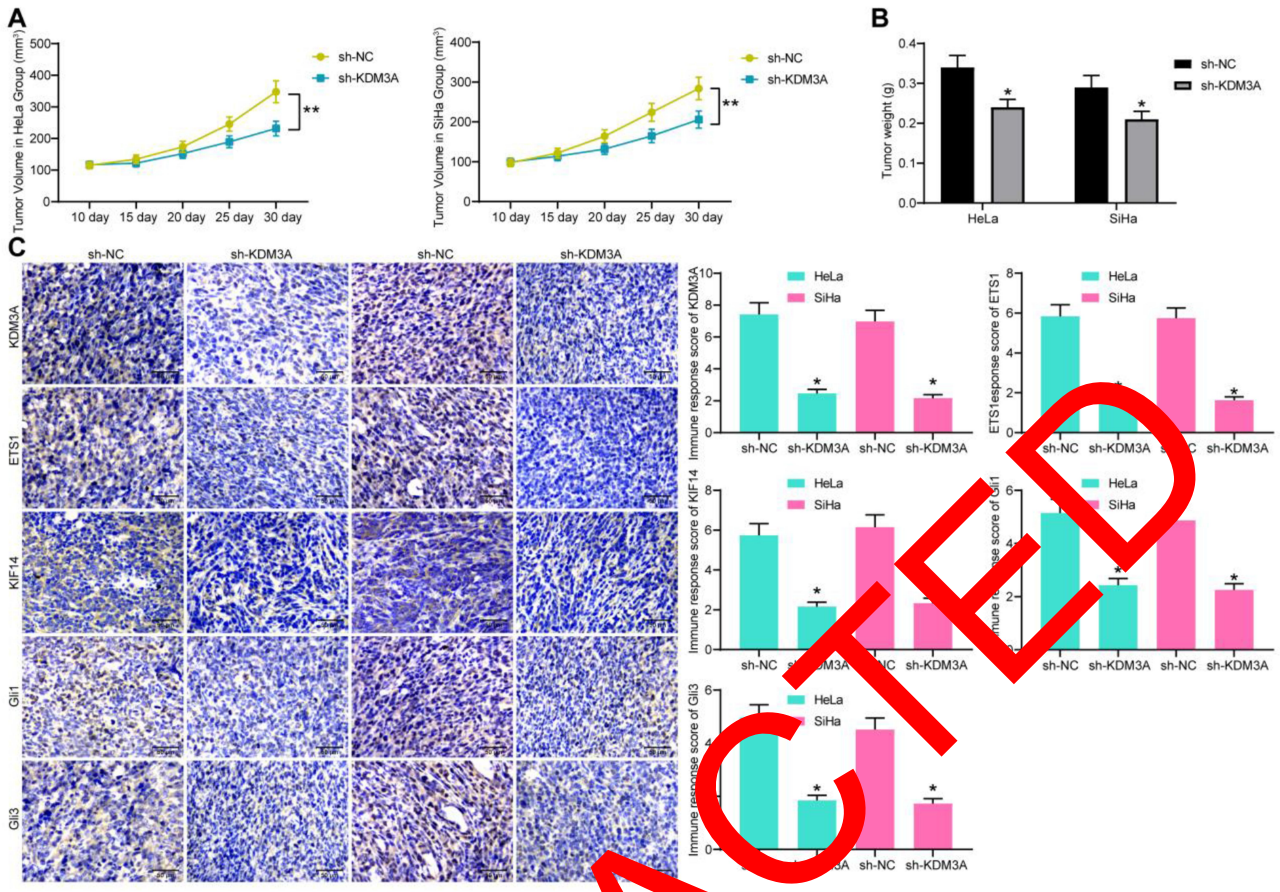

Figure 9 Sh-KDM3A suppresses tumor growth in vivo. (**A**) Tumor volume growth in mice by time (n=5); (**B**) weight of tumors in mice on the 30th day; (**C**) expression of *KDM3A*, *ETS1*, *KIF14*, Gli1, and Gli3 in tissues of xenograft tumors determined by IHC staining. Data were analyzed by one-way (panel **C**) or two-way (panels **A** and **B**) ANOVA. *P<0.05, **P<0.01 compared to sh-NC.

Similarly, abundant expression of *KDM3A* has been noted as an independent unfavorable factor in patients with pancreatic tumor[20] and colorectal cancer[24] and epithelial ovarian cancer.[25] A high-expression profile of *KDM3A* was also found in CC cell lines. In the following loss-of-function studies, we observed that sh-KDM3A suppressed growth and metastatic potential of HeLa and SiHa cells. In addition, an increase in the pro-apoptotic factor Bax and the epithelial marker E-cadherin while a decline in the anti-apoptotic factor Bcl-2 and mesenchymal markers N-cadherin and Vimentin suggested that sh-KDM3A promoted apoptosis while suppressing EMT in CC cells in a cellular perspective. In addition, angiogenesis, a hallmark of cancers that is crucial for tumor growth and metastasis,[26] was found to be suppressed as well upon KDM3A downregulation.

KDM3A catalyzes the demethylation of H3K9me1/me2 in vivo and in vitro with a preference for dimethylated residues, therefore governing transcriptional activation.[8,20,27,28] Intriguingly, studies have noted that *KDM3A* could control the transcriptional activation of *ETS1* in a similar manner.[9,29] *ETS1* has been noted as an important oncogene and a treating target in multiple malignancies including breast cancer,[30,31] ovarian cancer,[32,33] and CC as well.[11,34] To validate this potential interaction between *KDM3A* and *ETS1*, we first identified nuclear-localization of *KDM3A* and *ETS1* in CC cells, and then a positive correlation between *KDM3A* and ETS1 was identified. Further, the ChIP assays were performed, which suggested that *ETS1* promoter sequences were enriched by either anti-KDM3A or anti-H3K9me2. On this basis, we found that artificial overexpression of *ETS1* blocked the inhibitory roles of sh-KDM3A in CC cell growth, suggesting that *ETS1* is possibly responsible for the pro-oncogenic role of *KDM3A* in CC cells.

We then observed a positive relevance between *ETS1* and *KIF14* expression in the collected tissues and HeLa and SiHa cells. Then, the ChIP and luciferase assays suggested that as a transcription factor, *ETS1* had a direct binding relationship

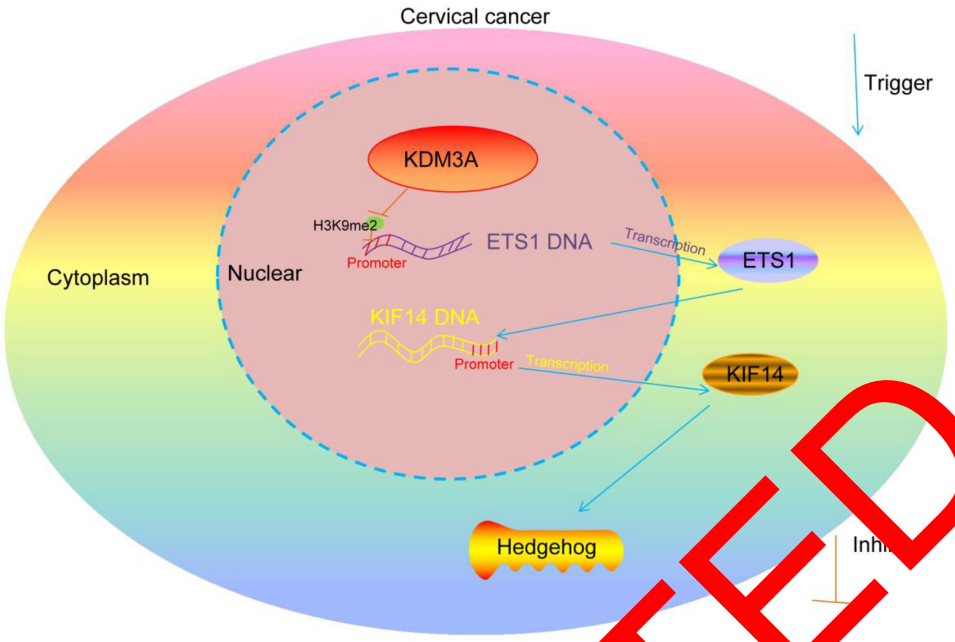

Figure 10 Diagram presentation of the molecular mechanism. *KDM3A* encourages the transcription of *ETS1* through the demethylation and histone modification of H3K9me2, while ETS1 further binds to the promoter region of *KIF14* to promote its transcription activity, which activate the Hedgehog signaling pathway and promote CC progression.

with the promoter sequence with *KIF14* and activated its transcription, which was partially in line with the previous report.[12] *KIF4* is a potent oncogene participating in the development of multiple cancers. For instance, it was associated with the metastasis and tumor progression as well as poor treating outcome in gastric cancer[35] and prostate cancer.[36] As for in CC, it was reported to predict distal prognosis and chemoresistance.[12] Here, after identification of the high-expression profile of *KIF14* in collected tissues, we noticed that overexpression of *KIF14* promoted the malignant behaviors of CC cells, which validated its oncogenic function in CC. Intriguingly, *KIF14* was documented as a positive regulator of the Hedgehog signaling pathway. Here, we found that KIF14 promoted the expression of Gli1 and Gli2 expression. This signaling pathway, first identified in fruit fly, is a highly conserved pathway responsible for signal transduction from cell membrane to nucleus, which plays crucial functions for embryonic development and is also implicated in cancer progression.[37–39] This is also applied in CC, where the Hedgehog was found to be correlated with radioresistance,[40] proliferation and survival,[41] and EMT and metastasis[16] of CC cells. Importantly, our study noticed that upregulation of the Hedgehog blocked the inhibitory functions of sh-KDM3A in CC cells, implicating its potential participation in *KDM3A*-mediated events. Consistently, similar results were reproduced in our in vivo experiments, where sh-KDM3A suppressed the growth of xenograft tumors in nude mice and the IHC staining intensity of *ETS1*, *KIF14*, Gil1, and Gil3 in the collected tumor tissues. To conclude, our experimental results provided evidence that *KDM3A* promotes CC growth in either cell and animal models through triggering *ETS1*-mediated *KIF14* transcription and the further upregulation the Hedgehog signaling pathway (Figure 10). This study may offer new understandings in CC progression and provide novel thoughts into CC treatment.

Data Sharing Statement

All the data generated or analyzed during this study are included in this published article.

Funding

There is no funding to report.

Disclosure

The authors declare no conflicts of interest in this work.

References

1. Bray F, Ferlay J, Soerjomataram I, Siegel RL, Torre LA, Jemal A. Global cancer statistics 2018: GLOBOCAN estimates of incidence and mortality worldwide for 36 cancers in 185 countries. *CA Cancer J Clin*. 2018;68(6):394–424. doi:10.3322/caac.21492

2. Shrestha AD, Neupane D, Vedsted P, Kallestrup P. Cervical cancer prevalence, incidence and mortality in low and middle income countries: a systematic review. *Asian Pac J Cancer Prev*. 2018;19(2):319–324.
3. Zheng J, Dai X, Chen H, Fang C, Chen J, Sun L. Down-regulation of LHPP in cervical cancer influences cell proliferation, metastasis and apoptosis by modulating AKT. *Biochem Biophys Res Commun*. 2018;503(2):1108–1114. doi:10.1016/j.bbrc.2018.06.127
4. Papatla K, Houck KL, Hernandez E, Chu C, Rubin S. Second primary uterine malignancies after radiation therapy for cervical cancer. *Arch Gynecol Obstet*. 2019;300(2):389–394.
5. Ayen A, Jimenez Martinez Y, Boulaiz H. Targeted gene delivery therapies for cervical cancer. *Cancers*. 2020;12:5. doi:10.3390/cancers12051301
6. Audia JE, Campbell RM. Histone modifications and cancer. *Cold Spring Harb Perspect Biol*. 2016;8(4):a019521. doi:10.1101/cshperspect.a019521
7. Wang T, Luo R, Li W, et al. Dihydroartemisinin suppresses bladder cancer cell invasion and migration by regulating KDM3A and p21. *J Cancer*. 2020;11(5):1115–1124. doi:10.7150/jca.36174
8. Yoo J, Jeon YH, Cho HY, et al. Advances in histone demethylase KDM3A as a cancer therapeutic target. *Cancers*. 2020;12:5. doi:10.3390/cancers12051098
9. Sechler M, Parrish JK, Birks DK, Jedlicka P. The histone demethylase KDM3A, and its downstream target MCAM, promote Ewing Sarcoma cell migration and metastasis. *Oncogene*. 2017;36(29):4150–4160. doi:10.1038/onc.2017.44
10. Dittmer J. The role of the transcription factor Ets1 in carcinoma. *Semin Cancer Biol*. 2015;35:20–38. doi:10.1016/j.semcancer.2015.09.010
11. Liao H, Pan Y, Pan Y, et al. MicroRNA874 is downregulated in cervical cancer and inhibits cancer progression by directly targeting ETS1. *Oncol Rep*. 2018;40(4):2389–2398.
12. Xu H, Zhao G, Zhang Y, et al. Long non-coding RNA PAXIP1-AS1 facilitates cell invasion and angiogenesis of glioma by recruiting transcription factor ETS1 to upregulate KIF14 expression. *J Exp Clin Cancer Res*. 2019;38(1):486. doi:10.1186/s13046-019-1474-7
13. Wang W, Shi Y, Li J, Cui W, Yang B. Up-regulation of KIF14 as a predictor of poor survival and a novel prognostic biomarker of chemoresistance to paclitaxel treatment in cervical cancer. *Biosci Rep*. 2016;36:2.
14. Pejskova P, Reilly ML, Bino L, et al. KIF14 controls ciliogenesis via regulation of Aurora A and is important for Hedgehog signaling. *J Cell Biol*. 2020;219:6. doi:10.1083/jcb.201904107
15. Wang YF, Yang HY, Shi XQ, Wang Y. Upregulation of microRNA-129-5p inhibits cell invasion, migration and tumor angiogenesis by inhibiting ZIC2 and downregulation of the Hedgehog signaling pathway in cervical cancer. *Cancer Biol Ther*. 2018;19(12):1162–1173. doi:10.1080/15384047.2018.1491497
16. Zhang F, Ren CC, Liu et al. SHH gene silencing suppresses epithelial-mesenchymal transition, proliferation, invasion, and migration of cervical cancer cells by repressing the Hedgehog signaling pathway. *J Cell Biochem*. 2018;119(5):3829–3842. doi:10.1002/jcb.26414
17. Che Y, Li Y, Zheng et al. TRIP4 promotes tumor growth and metastasis and regulates radiosensitivity of cervical cancer by activating MAPK, PI3K/AKT, and hTERT signaling. *Cancer Lett*. 2019;452:1–13. doi:10.1016/j.canlet.2019.03.017
18. Jiang C, Xu R, Li XX, et al. p53R2 overexpression in cervical cancer promotes AKT signaling and EMT, and is correlated with tumor progression, metastasis and poor prognosis. *Cell Cycle*. 2017;16(18):1673–1682.
19. Zeng YT, Liu XF, Yang WT, Zheng PS. REX1 promotes EMT-induced cell metastasis by activating the JAK2/STAT3-signaling pathway by targeting SOCS1 in cervical cancer. *Oncogene*. 2019;38(43):6940–6957. doi:10.1038/s41388-019-0906-3
20. Dandawate P, Ghosh C, Palaniyandi K, et al. The histone demethylase KDM3A, increased in human pancreatic tumors, regulates expression of DCLK1 and promotes tumorigenesis in mice. *Gastroenterology*. 2019;157(6):1646–1659 e1611. doi:10.1053/j.gastro.2019.08.018
21. He C, Yu L, Ding L, Yao H, Chen Y, Hao Y. Lysine demethylase KDM3A regulates nanophotonic hyperthermia resistance generated by 2D silicene in breast cancer. *Biomaterials*. 2020;255:120181. doi:10.1016/j.biomaterials.2020.120181
22. Ramadoss S, Guo G, Wang CY. Lysine demethylase KDM3A regulates breast cancer cell invasion and apoptosis by targeting histone and the non-histone protein p53. *Oncogene*. 2017;36(1):47–59. doi:10.1038/onc.2016.174
23. Ramadoss S, Sen S, Ramachandran I, Roy S, Chaudhuri G, Farias-Eisner R. Lysine-specific demethylase KDM3A regulates ovarian cancer stemness and chemoresistance. *Oncogene*. 2017;36(11):1537–1545. doi:10.1038/onc.2016.320
24. Liu J, Liang T, Zhangsun W. KDM3A is associated with tumor metastasis and modulates colorectal cancer cell migration and invasion. *Int J Biol Macromol*. 2019;126:[illegible]225. doi:10.1016/j.ijbiomac.2018.12.105
25. Yamada D, Kobayashi S, Yamamoto [illegible], et al. Role of the hypoxia-related gene, JMJD1A, in hepatocellular carcinoma: clinical impact on recurrence after hepatic resection, *Ann Surg Oncol*. 2012;19(3):S355–364. doi:10.1245/s10434-011-1797-x
26. Li X, Chen C, Dai Y, et al. Cinobufagin suppresses colorectal cancer angiogenesis by disrupting the endothelial mammalian target of rapamycin/hypoxia inducible factor 1alpha axis. *Cancer Sci*. 2019;110(5):1726–1734. doi:10.[illegible]11/cas.13988
27. Li Z, Xia J, Jiang [illegible], Xu Y. Epigenetic regulation of lung cancer cell proliferation and migration by the chromatin remodeling protein BRG1. *Oncogenesis*. 2019;8(11):66. doi:10.1038/s41389-019-0174-7
28. Mo LL, Peterle GT, Dos Santos M, et al. JMJD1A, H3K9me1, H3K9me2 and ADM expression as prognostic markers in oral and oropharyngeal squamous cell carcinoma. *PLoS One*. 2018;13(3):e0194884.
29. Sobo LM, Seiler M, Parrish JK, et al. KDM3A/Ets1/MCAM axis promotes growth and metastatic properties in Rhabdomyosarcoma. *Genes Cancer*. 2020;11(1–2):53–65.
30. Kim GE, Kwon HK, Lee CG, et al. Upregulation of Ets1 expression by NFATc2 and NFKB1/RELA promotes breast cancer cell invasiveness. *Oncogenesis*. 2018;7(11):91. doi:10.1038/s41389-018-0101-3
31. Wu M, Liu X, Jin W, et al. Targeting ETS1 with RNAi-based supramolecular nanoassemblies for multidrug-resistant breast cancer therapy. *J Control Release*. 2017;253:110–121.
32. Kleemann M, Schneider H, Unger K, et al. Induction of apoptosis in ovarian cancer cells by miR-493-3p directly targeting AKT2, STK38L, HMGA2, ETS1 and E2F5. *Cell Mol Life Sci*. 2019;76(3):539–559.
33. Tomar S, Plotnik JP, Haley J, et al. ETS1 induction by the microenvironment promotes ovarian cancer metastasis through focal adhesion kinase. *Cancer Lett*. 2018;414:190–204. doi:10.1016/j.canlet.2017.11.012
34. Kori M, Yalcin Arga K. Potential biomarkers and therapeutic targets in cervical cancer: insights from the meta-analysis of transcriptomics data within network biomedicine perspective. *PLoS One*. 2018;13(7):e0200717.
35. Yang Z, Li C, Yan C, et al. KIF14 promotes tumor progression and metastasis and is an independent predictor of poor prognosis in human gastric cancer. *Biochim Biophys Acta Mol Basis Dis*. 2019;1865(1):181–192. doi:10.1016/j.bbadis.2018.10.039
36. Zhang Y, Yuan Y, Liang P, et al. Overexpression of a novel candidate oncogene KIF14 correlates with tumor progression and poor prognosis in prostate cancer. *Oncotarget*. 2017;8(28):45459–45469. doi:10.18632/oncotarget.17564
37. Salaritabar A, Berindan-Neagoe I, Darvish B, et al. Targeting Hedgehog signaling pathway: paving the road for cancer therapy. *Pharmacol Res*. 2019;141:466–480. doi:10.1016/j.phrs.2019.01.014
38. Skoda AM, Simovic D, Karin V, Kardum V, Vranic S, Serman L. The role of the Hedgehog signaling pathway in cancer: A comprehensive review. *Bosn J Basic Med Sci*. 2018;18(1):8–20. doi:10.17305/bjbms.2018.2756

39. Xin M, Ji X, De La Cruz LK, Thareja S, Wang B. Strategies to target the Hedgehog signaling pathway for cancer therapy. *Med Res Rev*. 2018;38(3):870–913. doi:10.1002/med.21482
40. Liu C, Wang R. The roles of hedgehog signaling pathway in radioresistance of cervical cancer. *Dose Response*. 2019;17(4):1559325819885293. doi:10.1177/1559325819885293
41. Samarzija I, Beard P. Hedgehog pathway regulators influence cervical cancer cell proliferation, survival and migration. *Biochem Biophys Res Commun*. 2012;425(1):64–69. doi:10.1016/j.bbrc.2012.07.051